ORIGINAL ARTICLE
DOI: https://doi.org/10.18599/grs.2020.3.62-68
Russian Original 2020. Vol. 22. Is. 3. Pp. 62–68

Petro-elastic modeling deliverables for the Kharyaga Permian carbonate deposits

S.I. Gusev
ZARUBEZHNEFT-Dobycha Kharyaga LLC, Moscow, Russian Federation
E-mail: segusev@nestro.ru

Abstract. The purpose of this study is petro-elastic modeling of the Permian deposits occurring in the Kharyaga field, which is located in the Nenets Autonomous District of the Arkhangelsk Region and is confined to the Timan-Pechora Oil and Gas Province. The formations concerned are represented by the Artinskian and Asselian-Sakmarian deposits, which are mainly composed of carbonate sediments admixed with terrigenous material. At the first stage of the petro-elastic modeling, the initial data quality is evaluated, candidate wells are selected, logging curves for the target formation intervals are adjusted and normalized. After that, a comprehensive interpretation of the well logging data is carried out; reservoirs are identified; porosity and oil saturation are evaluated. At the next stage, a petro-elastic model is built, and analysis is carried out in order to understand whether or not reservoirs can be identified and to evaluate a saturation type within the range of elastic parameters. In such case, the elastic model is selected as a function of sedimentation and diagenetic processes, saturating fluid content, etc. As a result of the modeling process, reservoir/non-reservoir zoning was identified based on acoustic and shear impedance; a relationship between the acoustic impedance and porosity was also established. No correlation between the elastic parameters and the saturation type has been established, which may be attributable to hardness of the carbonate matrix and similar elastic properties of oil and water.

Keywords: petro-elastic modeling, well logging, porosity, acoustic impedance, shear impedance, oil saturation, carbonate reservoirs

Recommended citation: Gusev S.I. (2020). Petro-elastic modeling deliverables for the Kharyaga Permian carbonate deposits. *Georesursy = Georesources*, 22(3), pp. 62–68. DOI: https://doi.org/10.18599/grs.2020.3.62-68

Introduction

One of the methods to predict structural and reservoir properties is a seismic inversion that helps to evaluate lithological specifics, permeability and porosity, and saturation of the deposits concerned. At the same time, the seismic data inversion can be regarded as a deterministic or stochastic task that provides more opportunities to adapt the deliverables to a priory geological information.

The purpose of the seismic data inversion is to restore the following attributes: acoustic impedance, shear impedance and density. The next link between the elastic characteristics and permeability and porosity of the deposits is a petro-elastic model, which can be derived based on both theoretical and empirical data. For carbonate rock study, inclusion model can be used that approximates a rock as a homogeneous isotropic elastic body, which contains pore inclusions. Since the inclusions (pores) are less hard, as compared to minerals, they significantly impact general elastic rock properties. Such models are referred to as effective carbonate media models. Among the effective models, a differential effective model, self-consistent model, etc, are differentiated (Development of a petro-elastic modeling…, 2018).

The purpose of this study is to provide an assessment in order to understand whether or not the Kharyaga Permian deposits can be disaggregated by reservoirs/non-reservoirs and by saturation types within the elastic parameters range, based on the petro-elastic modeling method.

Given the task set, the following objectives are to be pursued (Sokolova, Popravko, 2012):

- To adjust, normalize and synthesize the logging curves;
- To analyze the main petro-elastic modeling methods and to select the best one;
- To build a petro-elastic model and analyze the effect of the saturation type on the logging curve response;
- To analyze the modeling deliverables and to support recommendations for further seismic inversion.

To pursue each of those objectives, a geoscience data

set was used including lithology and petrophysical study of the core samples, well logging and testing data. The modeling covered 10 wells, which drilled the Permian deposits and had the most representative logs. For the data processing, the Paradigm's Geolog 18 software was used.

General field information

The Kharyaga oil field is located in the Nenets Autonomous District of the Arkhangelsk Region and is confined to the Timan-Pechora Oil and Gas Province.

The formations concerned include the Artinskian (P1ar) and Asselian-Sakmarian (P1a+s) deposits. The main source minerals of P1ar consist of quartz (49%) and calcite (41%). The grain size distribution analysis carried out for the core samples taken from P1ar shows that the sandstone fraction in the rock matrix is marginal (less than 3%). A share of the siltstone fraction exceeds 30%. Hence, the P1ar reservoirs are represented by argillaceous siltstones. Artinskian calcite serves as cement. Porous-type reservoirs are of primary occurrence in the P1ar deposits.

The mineral analysis of the core samples has shown that calcite is the main source mineral in P1a+s – its average concentration is 93.5%. The carbonate cross-section of P1a+s features the presence of reservoirs that have complex pore geometry (Estimation of geological reserves…, 2017).

Logging curves normalization

The first stage of the petro-elastic modeling was to evaluate the quality of the logging curves used, to normalize and to restore the curves in the wash-out and log skip intervals. As the method to normalize the curves, a method was selected that enabled comparison of the curves distribution in the pay zone interval, as there was no marker formation, which lithology, petrophysical and stress-strain characteristics had been confirmed. All the studied wells are located within one pad, and, therefore, this rules out variability of the pay zone lithology and petrophysical characteristics that may be driven by the in-fill trend or lateral variability. The bar charts, which were built for all the studied wells, have shown that some of the wells feature a considerable deviation of the median value, as compared to main data selected (Figure 1):

The neutron porosity, bulk density, S and P-wave travel time curves in the wash-out and log skip intervals were adjusted based both on two-dimensional (Figure 2) and multi-dimensional petrophysical relationships with other (neutron and induction log) curves, and on empiric equations, like Gardner-Castagna relationship (equation 1) and Greenberg-Castagna relationship (equation 2) for pure limestones (Gardner, 1974). The curves were normalized, as a rule, through additive correction.

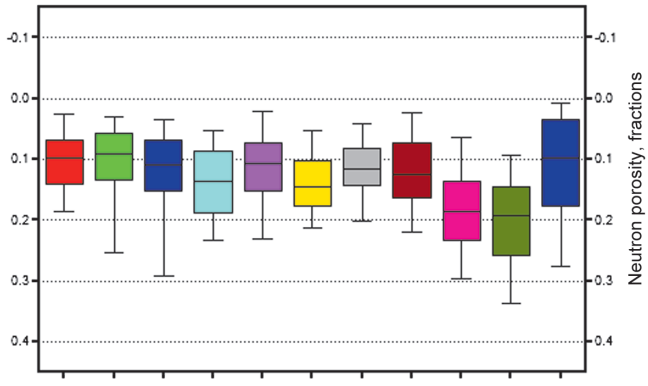

Fig. 1. Neutron porosity distribution in the pay zones before the logging curves were normalized and adjusted. The color represents different wells.

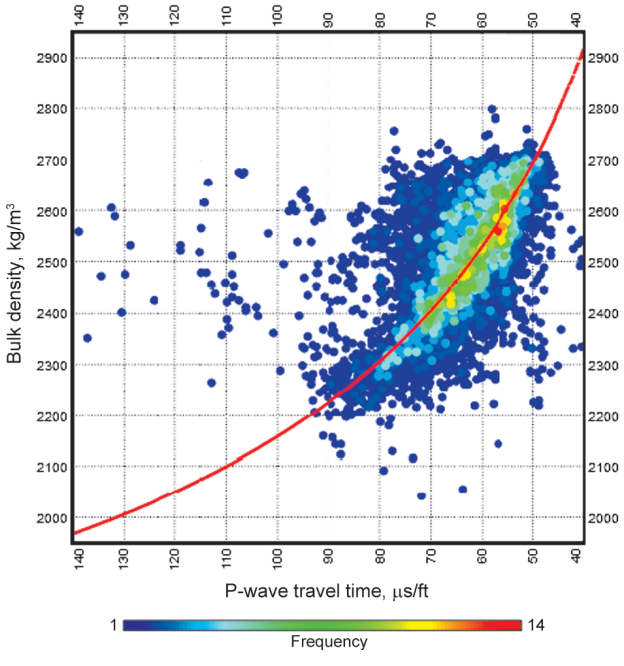

Fig. 2. Density vs. travel time

$$\rho = -0.0296 \cdot Vp^2 + 0.461 \cdot Vp + 0.963, \quad (1)$$

$$Vs = a \cdot Vp - b, \quad (2)$$

where ρ – rock density, g/cm^3; V_p – P-wave travel time, km/s; and V_s – S-wave travel time, km/s.

An example showing a restored P-wave travel time curve is presented in Figure 3.

An example of normalized bar charts showing neutron porosity distribution is presented in Figure 4.

Log interpretation

The next stage includes a comprehensive interpretation of the well logging data; reservoirs identification; porosity and oil saturation evaluation. To accomplish this task, a linear and nonlinear equation method was used to trace a relationship between physical properties of the minerals and fluids and the logging curves response. Such approach, for instance, has been implemented in the Multimin module of the Geolog 18 software. Based

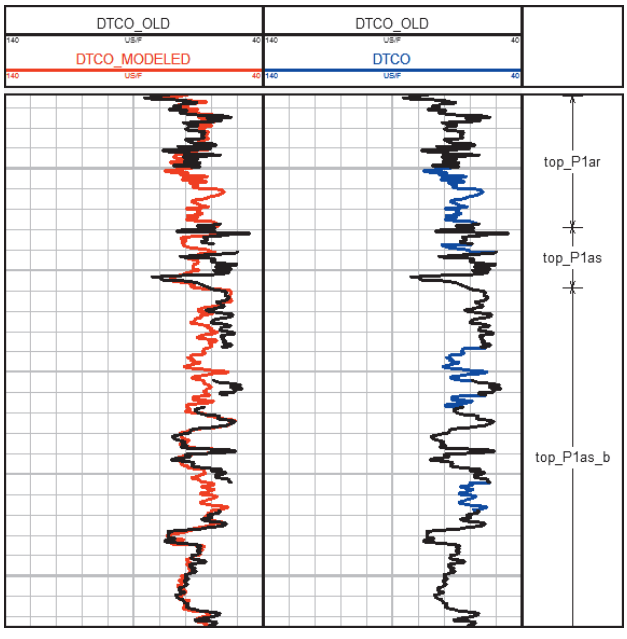

Fig. 3. An example showing a restored P-wave travel time curve for log skip intervals. The colors represent the following: black indicates a recorded log curve; red indicates a synthetic curve, blue indicates a restored curve for the log skip intervals.

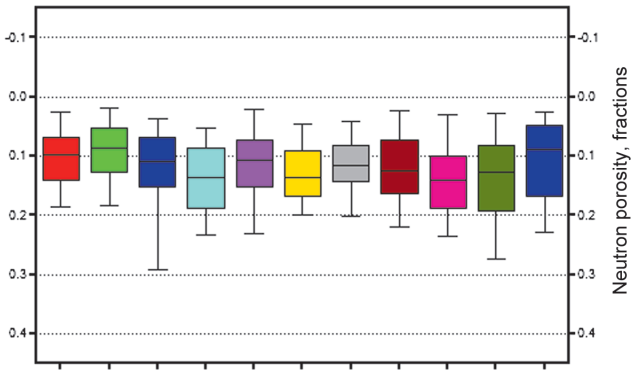

Fig. 4. Neutron porosity distribution in the pay zones after the logging curves were normalized and adjusted. The color represents different wells.

on the lithology and petrophysical study of the core and mud logs from the wells drilled, calcite, illite and quartz were selected as minerals to be simulated. Oil and water were selected as the pore fill. The following parameters were selected as arrival curves for the Multimin module: bulk density, neutron porosity calibrated to the limestone matrix, P-wave travel time, photoelectric factor, natural radioactivity, resistance in the washed-out and non-logged zones of the reservoir. To calculate the saturation, the Archie-Dakhnov equation was used, with the m and n factors being derived based on the core study. The produced water resistance was calculated based on salinity of samples taken, considering the reservoir temperature effect (Petersilier, 2003)

As a result, mineral models were derived, and fluids distribution was identified within the studied Artinskian and Asselian-Sakmatian deposits for each of the wells on the pad concerned. The reservoirs were identified based on cut-off porosity for each of the formations. The cut-off porosity was determined based on comprehensive core analysis, WFT, DST and formation testing data. A saturation type was determined based on the water saturation cut-off value, taking into account the accepted OWC (Figure 5).

As validation criteria for the resulting petrophysical model, the core data were used. Unfortunately, no core study data are available for the wells from this pad, which makes the direct comparison difficult. However, a lot of core studies have been run for the Artinskian and Asselian-Sakmarian deposits throughout the field, and given the consistency and regularity of permeability and porosity across the area, the relevant generalized average values can be used for comparison.

To study P1ar permeability and porosity, 682 core samples from 30 wells were used, out of which 171 samples represent reservoirs. P1ar porosity, which was measured on standard samples using the NaCl saturation method, varies from 0.3% to 37%, with the average value being 10.8%. The porosity in P1ar reservoirs varies between 14% and 37%; with the average reservoir porosity for 171 samples being 19.8%.

According to the logs, the average porosity in the Artinskian reservoirs is 20.3% (Figure 6).

To study P1a+sr permeability and porosity, 1336 core samples from 32 wells were used. P1a+s consists of the lower and upper layers. The upper layer has enhanced

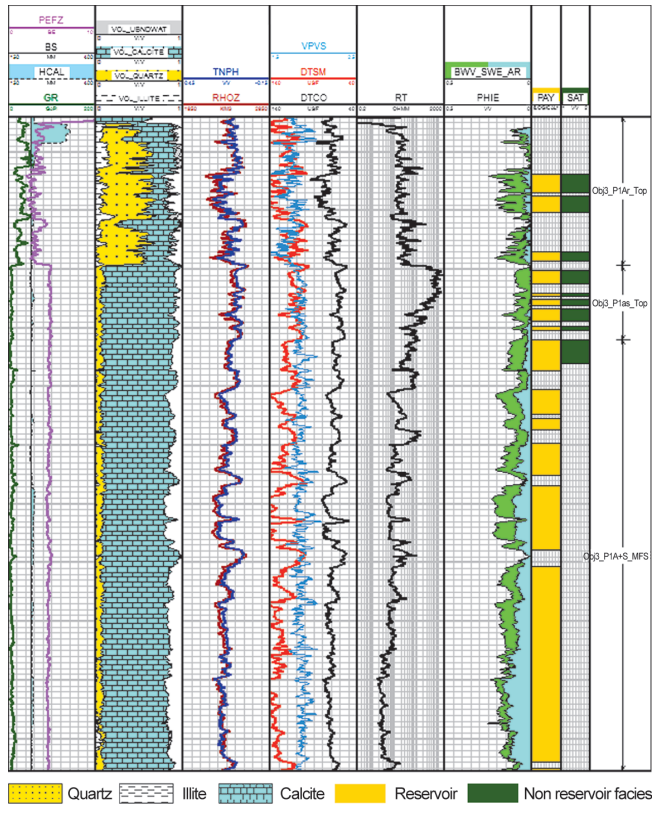

Fig. 5. An example of a petrophysical model built for one of the wells

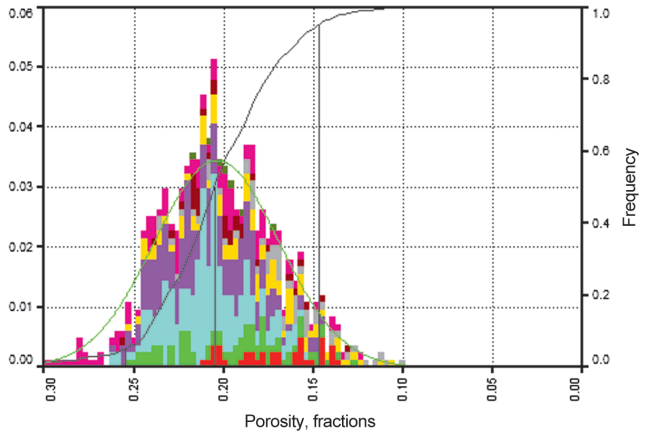

Fig. 6. Porosity distribution in the Artinskian deposits as per the logs. The color represents different wells.

reservoir properties. P1a+s permeability and porosity have been considered both as part of one single Object and by separate layers.

P1a+s porosity, which was measured on standard samples using the NaCl saturation method, varies from 0.29% to 26.6%, with the average value being 10.12%. The porosity in the upper layer of P1a+s varies between 8% and 26.6%; with the average reservoir porosity for 246 samples being 13.56%. The porosity in the lower layer of P1a+s varies between 11% and 24.6%; with the average reservoir porosity for 375 samples being 15.7%.

According to the logs, the average reservoir porosity in the upper layer of P1a+s is 11.9%, and that in the lower layer is 16.7%.

Hence, a conclusion can be reached that the resulting petrophysical model is consistent. Apart from that, the reservoir intervals and the estimation of the reservoir saturation were confirmed by the data from repeatable/wireline formation tests run in 4 wells and by the cased hole test data.

Petro-elastic modeling

At the next stage, a petro-elastic model is built, and analysis is carried out in order to understand whether or not reservoirs can be identified and to evaluate a saturation type within the range of elastic parameters. When selecting a model, the following specific features of the carbonate deposits should be considered (Development of a petro-elastic…, 2018):

Nonlinear relationship between porosity and elastic parameters, which is attributable to the impact of the pore geometry in the carbonate rocks;

Slight impact of the fluid type on the wave speed, which is attributable to the high hardness of the matrix;

The carbonate reservoir quality is not necessarily attributable to high porosity. Reservoir permeability and fluid filtration depend on the presence of fractures.

The multiple use of P- and S-waves velocities is such case is not so efficient, as compared to terrigenous rocks. The Poison's ratio, as a rule, slightly changes.

After the compressibility, density and P-wave travel time moduli for oil and water were determined, those parameters were also calculated for a fluid mixture, taking into account the actual oil saturation of the formations, based on a homogeneous mixing model, where the effective compressibility modulus is estimated based on the Reuss average (equation 3):

$$\frac{1}{K_{fl}} = \frac{S_1}{K_1} + \cdots + \frac{S_i}{K_i}, \quad (3)$$

where K_{f1} – fluid mixture compressibility modulus; K_i – compressibility modulus for the i-th component of the mixture; and S_i – saturation by the i-th component.

Based on the 3D mineral model resulting from the data interpretation, density, P- and S-wave velocities, Poisson's ratio, compressibility and shear moduli, as well as Voight upper bound and Royce low bound for the mineral mixture were calculated.

The resulting parameters were used for simulation of the elastic properties in a saturated rock, based on the effective differential model, with allowance made for various aspect ratios of the pore volume in the Artinskian and Asselian-Sakmarian deposits. The match between the simulated P- and S-wave travel time and density curves and the actual open hole log data was used as a validity criterion for the modeling (Figure 7). The resulting variance between the recorded and simulated logging curves does not normally exceed 5% and may be attributable to the source data quality.

The resulting petro-elastic model can not only simulate the impact of the permeability and porosity change on the elastic parameters, but can also predict the impact of a change in the reservoir saturation type on the elastic parameters, and, as consequence, on the seismic

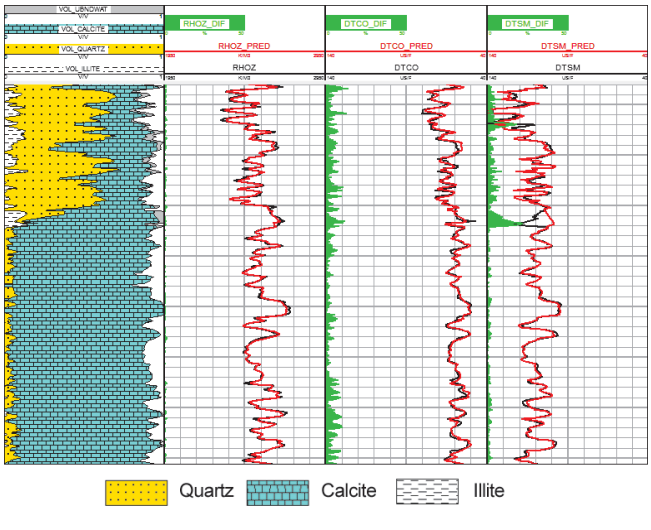

Fig. 7. Recorded vs simulated values of bulk density, P- and S-wave travel time. The black color represents the recorded logging curves, the red color represents the simulated curves, and the green color displays the percentage variance.

response, based on the Gassmann theory (equation 4) (Batzle, Wang, 1992).

$$\frac{K_{sat}}{K_0 - K_{sat}} = \frac{K_{dry}}{K_0 - K_{dry}} + \frac{K_{fl}}{phi \cdot (K_0 - K_{fl})} \quad (4)$$

where K_{dry} – dry rock compressibility modulus; K_{sat} – saturated rock compressibility modulus; K_o – composing mineral mixture compressibility modulus; K_{fl} – fluid mixture compressibility modulus; and *phi* — porosity.

To determine elastic characteristics that can be used for disaggregation by reservoirs/non-reservoirs and by saturation types, cross-plots and distribution bar charts were built.

Following the study completed, disaggregation by reservoir/non-reservoir was confirmed based on acoustic and shear impedance at the scale used for petrophysical data (Figures 8–9).

Relationship between acoustic, shear impedances and porosity was identified. This is a linear relationship, which depends on a type of a pore fluid (Figure 10).

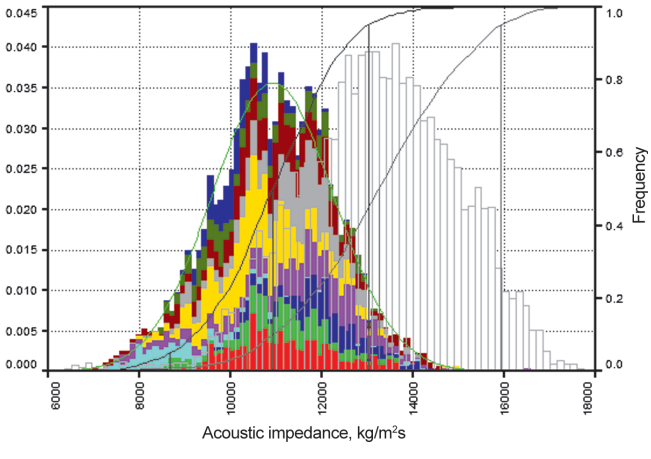

Fig. 8. Disaggregation by reservoir/non-reservoir based on acoustic impedance. The color fill indicates the reservoir (the color represents different wells), the transparent fill indicates the non-reservoir.

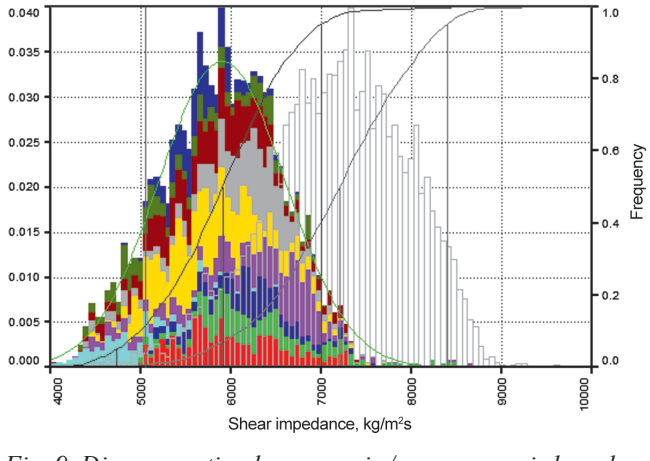

Fig. 9. Disaggregation by reservoir / non-reservoir based on shear impedance. The color fill indicates the reservoir (the color represents different wells), the transparent fill indicates the non-reservoir.

The elastic parameters do not differ a lot by a saturation type, and this was confirmed both by the actual data and by the simulation results (Figures 11–12), which makes it impossible to determine cut-off parameters to be able to identify a saturation type, using the seismic data.

As seen from Figure 11, the change in the saturation type from water to oil results in typical decrease in bulk density and P-wave velocity. The P-wave velocity

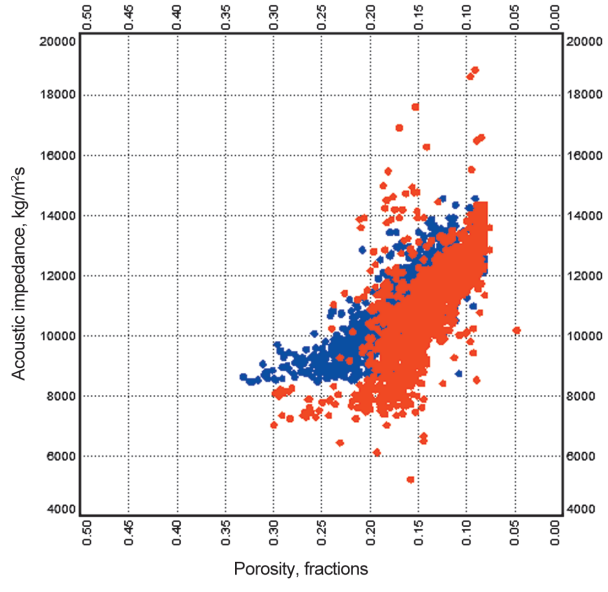

Fig. 10. Acoustic impedance vs. porosity for oil saturated and water saturated reservoirs. The blue and red colors accordingly represent water saturated and oil saturated reservoirs.

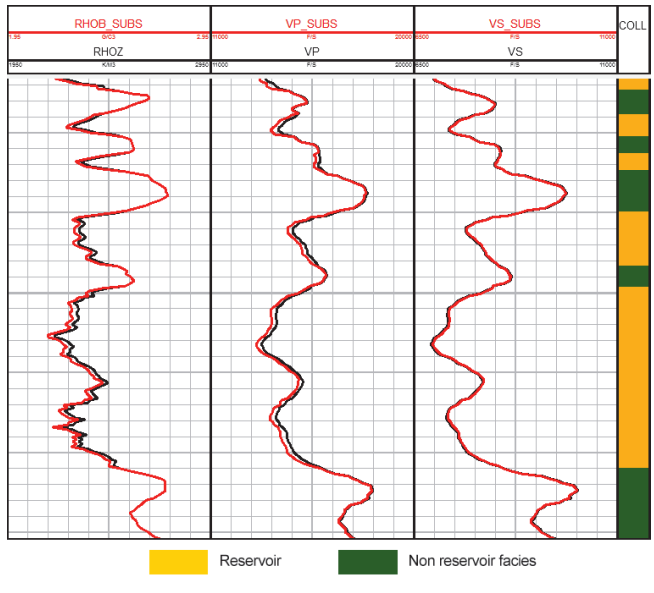

Fig. 11. An example showing simulation of the reservoir saturation type change from water to oil in one of the wells. The colors represents the following: black displays the logging curves recorded in the water saturated section of the formation; red displays displacement of water with oil after simulation; RHOB – bulk density, VP – P-wave velocity, VS – S-wave velocity, yellow fill displays the reservoir intervals; the green fill shows compact varieties.

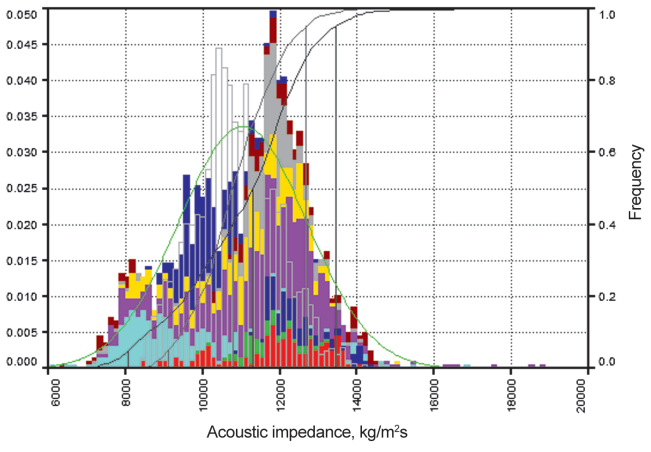

Fig. 12. Acoustic impedance distribution by saturation type. The color fill indicates water saturated reservoirs (the color represents different wells), the transparent fill indicates oil saturated reservoirs.

however does not almost change, which is confirmed by the physics of the method.

Apart from that, to study the lithology impact on the elastic characteristics of the deposits, relationship was plotted between the volumetric content of calcite in the rock matrix and density, P- and S-wave travel time.

The actual data confirmed the linear relationship between the volume of calcite, illite and quartz in the rock and the bulk density in the Artinskian and Asselian-Sakmarian deposits.

The relationship between the lithology and P- and S-wave travel time takes different forms for the Artinskian and Asselian-Sakmarian deposits, which can be illustrated in Figure 13.

The modeling of the logging curves response as a function of different calcite and quartz content in

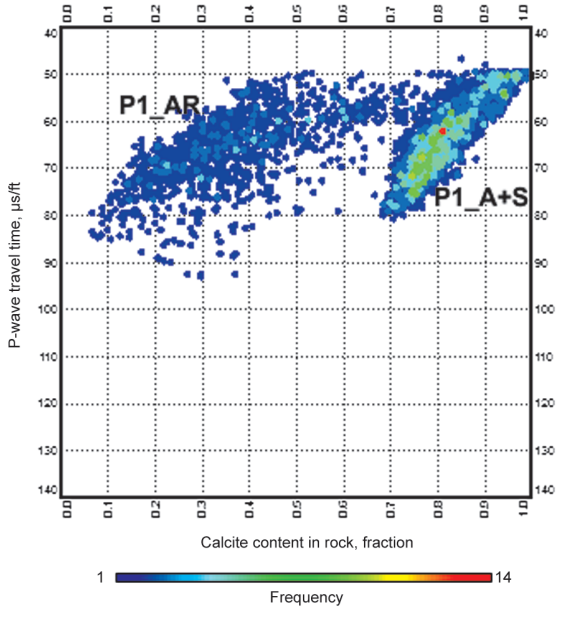

Fig. 13. Relationship between the P-wave travel time and calcite volume in rock

rock supports the assumption that variability in the relationships between the S-wave travel time and calcite content in the rock matrix may be explained not only by non-linear petrophysical equation, but also by the impact of Atrinskian shales and calcite cement on the P- and S-wave speed.

Such conclusion confirms the need to use at least 3 different minerals (quartz, illite, and calcite) when building a 3D petrophysical and petro-elastic model, and the need to use different aspect ratios of the pore volume for the Artinskian and Asselian-Sakmarian deposits, given the difference in the pore geometry and in intergranular cement properties.

Conclusion

Based on the petro-elastic modeling of the Kharyaga Permian deposits, it was established that they can be disaggregated by reservoirs/non-reservoirs using the acoustic and shear impedance; AVO/AVA inversion (Amplitude Versus Angle/Offset) was also found applicable to evaluation of porosity in the space between the wells. It was also established that there was no disaggregation by a saturation type, which may be attributable to the fact that water and oil have similar properties (density, travel time), as well as to the high hardness of the carbonate rock matrix, which alters the effect of the saturating fluid. These results are correlated with the Gubkin Russian Oil and Gas University experts' conclusions that have been made following the study of the Devonian carbonate deposits at the West Khosedayu field (Development of a petro-elastic…, 2018).

Given the fact that the ultimate objective of the petro-elastic modeling procedure is to predict the lithology and reservoir properties of the Kharyaga Permian carbonate deposits, the main efficiency criterion for the petro-elastic modeling will be the match between predicted and actual data. As the actual data, information from both new wells and from wells, which have not been used for the simulation process (reference well), may be used. Apart from that, the resulting volumes and maps showing the lithology and petrophysical properties distribution, shall be compliant with the accepted geological concept. For instance, in case of reef sequences, the lateral distribution of the reef facies shall have a well defined shape, depending on a type of the reef structures genesis.

Hence, a conclusion may be reached that these findings serve as prerequisites for using the seismic data inversion in order to predict the reservoirs distribution throughout the Kharyaga field and to evaluate their porosity. The inversion and evaluation of the findings obtained constitute the next stage of the study to predict lateral distribution of the reservoirs and to evaluate their permeability and porosity.

References

Batzle M, Wang Z. (1992). Seismic properties of pore fluids. *Geophysics*, 57, pp. 1396-1408. https://doi.org/10.1190/1.1443207

Development of a petro-elastic modeling technique for predicting the lithology and reservoir properties of carbonate deposits of the West Khosedayu deposit. (2018). Moscow: Gubkin Russian State University of oil and gas.

Estimation of geological reserves of oil, dissolved gas and associated components of the Kharyaga oil field. (2017). Moscow: VNIIneft.

Gardner G.H.F. (1974). Formation velocity and density – The diagnostic basics for stratigraphic traps. *Geophysics*, 39, pp. 770-780. https://doi.org/10.1190/1.1440465

Petersilie V.I. (2003). Guidelines for calculating the geological reserves of oil and gas by the volumetric method. Moscow-Tver, 259 p.

Sokolova T.F., Popravko A.A. (2012). Problems of modeling the elastic properties of rocks according to geophysical research of wells for seismic inversion. *Collected papers UkrGRI,* 4, pp. 139-157.

About the Author

Sergey I. Gusev – Head of Well Logging Section, ZARUBEZHNEFT-Dobycha Kharyaga LLC

3 Paveletskaya square, build. 2, Moscow, 115054, Russian Federation

Manuscript received 12 November 2020;
Accepted 2 July 2020; Published 30 September 2020